



Influence of titanium dioxide nanoparticles on the transport and deposition of microplastics in quartz sand[☆]

Li Cai^{a, b, 1}, Lei He^{a, 1}, Shengnan Peng^a, Meng Li^a, Meiping Tong^{a, *}

^a The Key Laboratory of Water and Sediment Sciences, Ministry of Education, College of Environmental Sciences and Engineering, Peking University, Beijing, 100871, PR China

^b Natural History Research Center, Shanghai Natural History Museum, Shanghai Science and Technology Museum, Shanghai, 200127, PR China

ARTICLE INFO

Article history:

Received 9 February 2019

Received in revised form

27 June 2019

Accepted 2 July 2019

Available online 9 July 2019

Keywords:

Microplastic

$n\text{TiO}_2$

Transport

Deposition

Quartz sand

ABSTRACT

The influence of titanium dioxide nanoparticles ($n\text{TiO}_2$) on the transport and deposition of polystyrene microplastics (MPs) in saturated quartz sand was investigated in NaCl solutions with ionic strengths from 0.1 to 10 mM at two pH conditions (pH 5 and 7). Three different-sized polystyrene (PS) MPs (diameter of 0.2, 1, and 2 μm) were concerned in present study. We found that for all three different-sized MPs in NaCl solutions (0.1, 1 and 10 mM) at both pH 5 and 7, lower breakthrough curves and higher retained profiles of MPs with $n\text{TiO}_2$ copresent in suspensions relative to those without $n\text{TiO}_2$ were obtained, demonstrating that the copresence of $n\text{TiO}_2$ in MPs suspensions decreased MPs transport and increased their deposition in quartz sand under all examined conditions. The mechanisms contributing to the increased MPs deposition with $n\text{TiO}_2$ in suspensions at two pH conditions were different. The formation of MPs- $n\text{TiO}_2$ heteroaggregates and additional deposition sites provided by previously deposited $n\text{TiO}_2$ were found to drive to the increased MPs deposition with $n\text{TiO}_2$ in suspensions at pH 5, while the formation of MPs- $n\text{TiO}_2$ aggregates, additional deposition sites and increased surface roughness induced by the pre-deposited $n\text{TiO}_2$ on quartz sand surfaces were responsible for the enhanced MPs deposition at pH 7. The results give insights to predict the fate and transport of different-sized MPs in porous media in the copresence of engineered nanoparticles.

© 2019 Elsevier Ltd. All rights reserved.

1. Introduction

Various applications of plastics in commercial products induced ubiquitous plastic pollution in natural environments (Cheung and Fok, 2016; Eerkes-Medrano et al., 2015; Napper and Thompson, 2016; Zhang et al., 2017). Microplastics (MPs) with size ranging from 100 nm to 5 mm were found to be ubiquitously present in environmental systems (Alimi et al., 2018). In addition to the primary MPs discharged from personal care products (Hernandez et al., 2017; Napper and Thompson, 2016), secondary MPs in natural environments are produced by mechanical abrasion, UV radiation, weathering and biodegradation (Ivleva et al., 2017; Ter et al., 2016). The plastic production processes via the polymerization of various monomers and additives resulted in the presence of

different functional groups such as COO^- , CH_3^- , NH_2^- , $\text{C}=\text{C}^-$, SO_3H on the surfaces of MPs (Wang et al., 2018). Due to the adsorption of pollutants such as heavy metals (Brennecke et al., 2016; Turner, 2016) and persistent organic pollutants (Rochman et al., 2014; Wardrop et al., 2016) on their surfaces, MPs thus have been shown to have potential threat to natural ecosystems and even to human health, which have been identified as contaminants of emerging concerns in both aquatic and terrestrial environments (Browne et al., 2007; de Souza Machado et al., 2018; Li et al., 2016).

Once released into the aquatic environments, MPs are likely to interact with other substances such as colloids and ions present in natural environment and thus their fate and transport in environment would be altered. Several studies have been performed to explore the aggregation and transport of MPs in different conditions (e.g. Cai et al., 2018; Dong et al., 2019; Li et al., 2018; Li et al., 2019). For instance, Li et al. (2018) found that humic acid could enhance the stability of polystyrene (PS) and decreased their aggregation. Cai et al. (2018) showed that Fe^{3+} could induce the aggregation of nanoplastics (NPs). Dong et al. (2019) recently found that the different effects of fullerene on NPs transport in marine

[☆] This Paper has been recommended for acceptance by Rong Ji.

* Corresponding author.

E-mail address: tongmeiping@pku.edu.cn (M. Tong).

¹ These authors contribute equally to this article.

environments were governed by the mass concentration ratio of NPs/fullerene. Very recently, Li et al. (2019) reported that goethite and hematite (both positively charged) could decrease the transport of MPs with different sizes via different mechanisms. Due to the unique characteristics, various engineered nanomaterials were synthesized and have been applied in different fields (Erickson, 2012; Mueller and Nowack, 2010). As very important metal oxide nanoparticles, titanium dioxide nanoparticles ($n\text{TiO}_2$) are used in different types of fields such as cosmetics industry, textile industry, as well as water treatment processes (Gottschalk et al., 2013; Keller and Lazareva, 2013). The increasing $n\text{TiO}_2$ applications will release $n\text{TiO}_2$ into environmental systems (Lin et al., 2010; Mueller and Nowack, 2008). It is highly likely that MPs and $n\text{TiO}_2$ particles could interact with each other after they encounter in environments, thus the fate and transport of MPs in natural environments might be altered by the copresence of $n\text{TiO}_2$. However, the effects of $n\text{TiO}_2$, especially with different surface charge, on the transport and deposition behaviors of MPs in porous media have not been previously examined. The corresponding mechanisms dominating the MPs transport with the copresence of $n\text{TiO}_2$ thus remain unclear. It is worth pointing out that although a few previous studies have investigated the cotransport of $n\text{TiO}_2$ with other colloidal particles such as fullerene (Cai et al., 2013) and multi-walled carbon nanotubes (Wang et al., 2014), as well as the cotransport of MPs with other colloids such as iron oxides (Li et al., 2019) and fullerene (Dong et al., 2019), yet the mechanisms dominating the cotransport behaviors varied for different systems. Thus, the results obtained from these previous studies might not apply to the transport of MPs with the copresence $n\text{TiO}_2$ in suspensions. To fully understand the fate and transport of MPs in a more realistic environment with copresence of $n\text{TiO}_2$, further studies regarding the mechanisms dominating MPs transport with $n\text{TiO}_2$ are definitely required.

In this study, the effects of $n\text{TiO}_2$ (with either positive or negative surface charges) on the transport and deposition of MPs in packed quartz sand were systematically examined. Polystyrene particles, one type of plastics widely present in natural environments (Alimi et al., 2018; Pitt et al., 2018), were used as model MPs. Three different-sized MPs (0.2, 1, and 2 μm) were concerned in present study. MPs transport experiments both with and without $n\text{TiO}_2$ in MPs suspensions were conducted at three ionic strengths (0.1, 1 and 10 mM) in NaCl solutions at both pH 5 and 7. Possible mechanisms controlling the transport and deposition of MPs at different pH conditions were proposed and discussed. The results give insights to assess the environmental fate and ecological risks of MPs in natural systems.

2. Methods and materials

2.1. MPs and titanium dioxide suspension preparation

Three different-sized polystyrene latex microspheres (diameter of 0.2, 1, and 2 μm) with carboxylic functional groups (Molecular Probes, Invitrogen Canada Inc.) were used as model MPs in all experiments. Anatase titanium dioxide powders (purity greater than 99.7%, catalog # 637254) obtained from Sigma-Aldrich Corp. were employed to prepare $n\text{TiO}_2$ suspension. The detailed method to prepare MPs and $n\text{TiO}_2$ suspensions was given in Text S1 of Supplementary Information.

The influent mass concentration of $n\text{TiO}_2$ and all three different-sized MPs for all column experiments were maintained to be 50 mg L^{-1} and $\sim 4 \text{ mg L}^{-1}$, respectively (the number concentrations of 0.2, 1, and 2 μm MPs were 9×10^8 , 7.2×10^6 , and $9 \times 10^5 \pm 30\%$ particles mL^{-1}). The details about MPs concentration determination are given in the Supplementary Information (Text S2, Figs. S1 and S2). Three ionic strengths (0.1, 1 and 10 mM) in NaCl

solutions and two pHs (pH 5 and 7) were considered. Both zeta potentials and particle sizes of MPs and $n\text{TiO}_2$ under these conditions were determined by Zetasizer Nano ZS90 (Malvern Instruments, UK).

2.2. Column experiments

Cleaned quartz sand with sizes ranging from 417 to 600 μm were wet-packed into cylindrical Plexiglas columns with 2 cm inner diameter and 10 cm length. The detailed information about quartz sand cleaning and characterizing protocol, as well as column packing are provided in the Supplementary Information (Text S3 and Text S4). Packed quartz sand porosity was ~ 0.42 . Before the colloid transport experiments, more than ten pore volumes (10 PVs) of NaCl salt solutions were introduced into the column to pre-equilibrate the quartz sand. After that, 3 PVs of MPs suspensions both with and without the copresence of $n\text{TiO}_2$ were introduced into the column, which then eluted with 5 PVs of salt solution without MPs. Transport experiments were performed in up-flow mode with pore water velocity of 8 m day^{-1} (0.73 mL min^{-1}) in NaCl solutions (0.1, 1, and 10 mM) at two pH conditions (5 and 7). The influent suspension was adjusted to the desired pH before column experiments by using 0.1 M HCl or 0.1 M NaOH. Effluent suspensions during the transport experiments were sampled to yield the breakthrough curves. After the transport experiment, MPs were desorbed from quartz sand to yield the retained profiles. Details about MPs mass recovery can be found in the Supplementary Information (Text S4 and Table S1).

3. Results and discussion

3.1. Influence of $n\text{TiO}_2$ on the transport and deposition of MPs at pH 5

To determine the effects of positively charged $n\text{TiO}_2$ on the MPs transport behaviors, transport experiments of three different-sized MPs (0.2, 1 and 2 μm) both with and without $n\text{TiO}_2$ in quartz sand were performed in NaCl solutions (0.1, 1, and 10 mM) at pH 5. At all three ionic strengths at pH 5, the zeta potentials of all three different-sized MPs and quartz sand were negative (Table S2). Repulsive electrostatic interaction thus was present between MPs and quartz sand at pH 5 (Fig. S3), which resulted in the obvious breakthrough of MPs under all examined ionic strengths (Fig. 1, left, open symbol). Increasing solution ionic strength slightly decreased the zeta potentials of both MPs and quartz sand at pH 5 (Table S2), the interaction between MPs and quartz sand thus was less repulsive at high ionic strength relative to low ionic strength (Fig. S3). For all three sized MPs (0.2, 1 and 2 μm), their transport thus decreased with increasing ionic strength especially in 10 mM NaCl solutions, as shown by the lower breakthrough plateau at higher ionic strength. The decreased MPs transport with increasing ionic strength in porous media has also been reported previously (Dong et al., 2019; Li et al., 2018). With the copresence of $n\text{TiO}_2$ in suspensions under three ionic strengths in NaCl solutions, BTCs of all three different-sized MPs (Fig. 1, left, solid symbol) were lower than those without $n\text{TiO}_2$ (Fig. 1, left, open symbol) at pH 5. For example, $\sim 79\%$ of 1 μm MPs eluted from the columns without $n\text{TiO}_2$ in 1 mM NaCl solutions, whereas, 52% of 1 μm MPs broke through the columns with $n\text{TiO}_2$ copresent in suspensions at the same ionic strength condition. This observation demonstrated that at pH 5, $n\text{TiO}_2$ present in MPs suspensions could inhibit the transport of MPs (with three different sizes) in quartz sand.

To examine the distribution of MPs retained in quartz sand in the copresence of $n\text{TiO}_2$, the retained profiles of MPs under all ionic strength conditions at pH 5 were obtained, and the results are

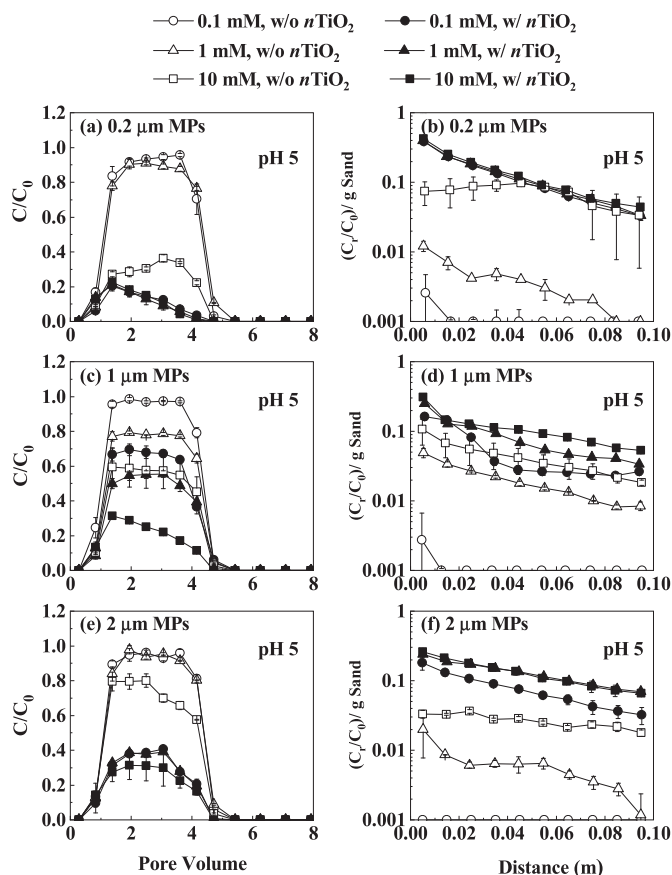


Fig. 1. Breakthrough curves and retained profiles of MPs (0.2, 1 and 2 μm) both with and without $n\text{TiO}_2$ in NaCl solutions (0.1, 1 and 10 mM) at pH 5.

provided in Fig. 1 (right). The retained profiles were the inverse of the plateaus of BTCs, as expected from mass balance considerations (Table S1). In the absence of $n\text{TiO}_2$, the retained concentrations of all three different-sized MPs were negligible in 0.1 mM at pH 5 (Fig. 1, right, open circle) due to their high mobility at this low ionic strength regardless of MPs sizes. The retained concentrations of MPs increased with increasing ionic strength, which was consistent with less zeta potentials at higher ionic strength (Table S2) and thus agreed with DLVO theory (Fig. S3). More important observation is that the concentrations of MPs retained in quartz sand with $n\text{TiO}_2$ copresent in suspensions (Fig. 1, right, solid symbol) were greater relative to those in the absence of $n\text{TiO}_2$ (Fig. 1, right, open symbol). This held true for all three different-sized MPs under all ionic strength conditions (0.1–10 mM) in NaCl solutions at pH 5. The observation clearly showed that the copresence of $n\text{TiO}_2$ in suspension increased the deposition of all three different-sized MPs in porous media under all examined solution conditions at pH 5.

Close inspection of MPs retained profiles in the presence of $n\text{TiO}_2$ at pH 5 revealed that the increased retention of MPs with the copresence of $n\text{TiO}_2$ occurred across the entire column yet with the largest portion retained near column inlet, which led to the change of the shape of MPs retained profiles with $n\text{TiO}_2$ (Fig. 1, right, solid symbol) versus those without the presence of $n\text{TiO}_2$ (Fig. 1, right, open symbol). The retained profiles of MPs with the copresence of $n\text{TiO}_2$ were mainly in the form of exponential decrease with increase transport distance, which was different from those without the presence of $n\text{TiO}_2$. The observation suggested that mechanisms controlling MPs deposition with the copresence of $n\text{TiO}_2$ differed from those without the presence of $n\text{TiO}_2$, detailed discussion was

provided below.

Previous studies (Dong et al., 2018; Legg et al., 2014; Xia et al., 2019) have shown that increasing colloidal sizes would increase their deposition in porous media. At pH 5, it is expected that positively charged $n\text{TiO}_2$ would interact with negatively charged MPs (Table S2 and Fig. S4) and MPs- $n\text{TiO}_2$ clusters would be formed. Comparing with the individual MPs, the relatively larger clusters of MPs- $n\text{TiO}_2$ heteroaggregates would be easier to be retained in quartz sand, leading to the decreased transport and increased deposition of MPs with $n\text{TiO}_2$ copresent in suspensions at pH 5. To directly observe the aggregation status of MPs with the copresence of $n\text{TiO}_2$ particles in suspensions, representative SEM image of 1 μm MPs and $n\text{TiO}_2$ mixture was obtained in 1 mM NaCl solutions at pH 5 (Fig. 2). It was clearly seen that $n\text{TiO}_2$ nanoparticles adsorbed onto surfaces of 1 μm MPs, resulting in the formation of large clusters (MPs- $n\text{TiO}_2$ heteroaggregates). Cai et al. (2013) also found when $n\text{TiO}_2$ were copresent with fullerene nanoparticles, the larger cluster of $n\text{TiO}_2$ - C_{60} was formed at pH 5. Furthermore, the particle sizes in MPs- $n\text{TiO}_2$ mixed suspensions were found to be larger than individual MPs (without copresence of $n\text{TiO}_2$ in suspensions) in both 1 and 10 mM NaCl solutions (Fig. S5). The larger particle sizes with copresence of $n\text{TiO}_2$ relative to those without $n\text{TiO}_2$ were more obvious at higher ionic strength with the relatively larger clusters present in 10 mM NaCl solutions. The observations indicated that large MPs- $n\text{TiO}_2$ clusters (with surface charge heterogeneity) were formed in MPs and $n\text{TiO}_2$ suspensions at pH 5. In addition, comparison of the size distribution of MPs (1 μm) with $n\text{TiO}_2$ copresent in suspensions in influent suspension versus effluent suspension showed that the particle size in influent suspension was larger than that in effluent suspension in 1 mM NaCl solutions at pH 5 (Fig. S6). The results suggested that during their transport through the columns, large clusters of MPs- $n\text{TiO}_2$ suspensions were retained in columns and thus led to the smaller sizes of MPs- $n\text{TiO}_2$ mixtures in effluent suspensions. Comparing with individual MPs with copresence of $n\text{TiO}_2$, the larger sized MPs- $n\text{TiO}_2$ clusters would be easier to be retained in quartz sand, resulting in the increased MPs deposition with copresence of $n\text{TiO}_2$ at pH 5.

Moreover, since $n\text{TiO}_2$ particles contained positive surface charge at pH 5, the charge heterogeneity thus would be present on the surfaces of MPs- $n\text{TiO}_2$ clusters, which would lead to the less repulsive interaction (even attractive interaction) between MPs- $n\text{TiO}_2$ clusters and quartz sand relative to that without $n\text{TiO}_2$. As a result, the larger MPs- $n\text{TiO}_2$ clusters with surface charge heterogeneity would be easier to be retained in quartz sand relative to the individual MPs, leading to the enhanced MPs deposition in the

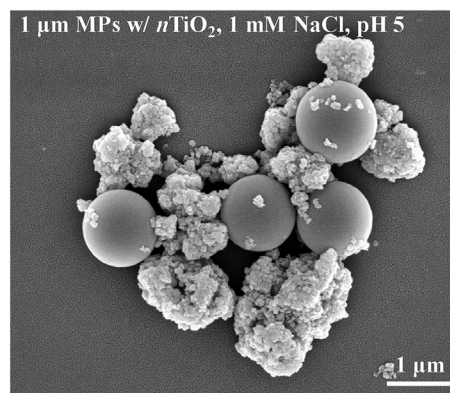


Fig. 2. SEM image of MPs (1 μm) and $n\text{TiO}_2$ mixed suspensions in 1 mM NaCl solutions at pH 5.

presence of $n\text{TiO}_2$ at pH 5. Previous studies (Bradford et al., 2007; Li et al., 2019; Tong and Johnson, 2007) also reported that the chemical heterogeneity on the surfaces of colloids could influence their transport and deposition in quartz sand.

Via pre-depositing onto surfaces of porous media, substances copresent in colloid suspensions would serve as additional sites for colloid deposition and thus could decrease colloid transport behaviors in porous media (Chen et al., 2012; Yang et al., 2016). Besides the interaction with MPs, positively charged $n\text{TiO}_2$ could also adsorb onto the quartz sand during the cotransport processes with MPs. It is more likely for MPs to deposit positively charged $n\text{TiO}_2$ that pre-adsorbed onto quartz sand rather than on the negatively charged quartz sand, resulting in the increased MPs deposition. To verify the contribution of additional deposition sites provided by the pre-deposited $n\text{TiO}_2$ nanoparticles on quartz sand surfaces to the decreased MPs transport with copresence of $n\text{TiO}_2$ at pH 5, additional column experiments were performed in 1 mM NaCl solutions. Specifically, 3 PVs of 50 mg L^{-1} $n\text{TiO}_2$ suspensions was introduced to pre-equilibrate the columns prior to the injection of $1 \mu\text{m}$ MPs suspensions. Results showed that MPs BTCs (~20% breakthrough) with $n\text{TiO}_2$ pre-equilibrating columns yet without the presence of $n\text{TiO}_2$ during MPs transport experiment (Fig. 3, solid diamond) were lower relative to those (~80% breakthrough) of individual MPs transport (Fig. 3, open triangle). The result suggested that when present in MPs suspensions, $n\text{TiO}_2$ pre-deposited onto quartz sand could attract more deposition of MPs via serving as additional sites at pH 5. Since the amount of $n\text{TiO}_2$ pre-deposited onto quartz sand surfaces during pre-equilibration process would be greater than that copresent in MPs suspensions, thus, MPs BTC for columns with $n\text{TiO}_2$ pre-treatment yet without $n\text{TiO}_2$ in MPs suspensions (Fig. 3, solid diamond) was lower than that only with $n\text{TiO}_2$ in MPs suspensions (without pre-treatment column) (Fig. 3, solid triangle). The increased attachment of negatively charged cells onto positively charged quartz sand coated with goethite (Kim et al., 2008) and increased deposition of negatively charged fullerene (Cai et al., 2013) and CNTs (Wang et al., 2014) onto $n\text{TiO}_2$ pre-deposited quartz sand have also been previously observed.

The above observations demonstrated that the combination of the formation of large MPs- $n\text{TiO}_2$ clusters (with surface heterogeneity) and the additional deposition sites provided by the positively

charged $n\text{TiO}_2$ pre-deposited on sand surfaces (the formation of collector heterogeneity) drove to the decreased MPs (with three different sizes) transport in the copresence of $n\text{TiO}_2$ in suspensions at pH 5. Previous studies reported that the colloid and or collector heterogeneity could shift the unfavorable colloid deposition to be favorable deposition condition, affecting the transport and retention of colloid in porous media (Chen et al., 2001; Elimelech et al., 2000; Yao et al., 1971). The chemical heterogeneity of MPs- $n\text{TiO}_2$ clusters and the positively charged $n\text{TiO}_2$ previously deposited onto the quartz sand would also lead to the presence of favorable deposition condition for MPs in the copresence of $n\text{TiO}_2$ at pH 5. As a result, the majority of retained profiles of MPs in the presence of $n\text{TiO}_2$ was in the form of the exponential decrease at pH 5, which agreed with classical filtration theory (CFT) (Yao et al., 1971).

3.2. Influence of $n\text{TiO}_2$ on the transport and deposition of MPs at pH 7

To investigate whether negatively charged $n\text{TiO}_2$ could also affect the transport behaviors of MPs in porous media, transport experiments of MPs with three sizes (0.2, 1 and $2 \mu\text{m}$) both with and without $n\text{TiO}_2$ copresent in suspensions in quartz sand were examined in NaCl solutions (0.1, 1 and 10 mM) at pH 7. The zeta potentials of both MPs (0.2– $2 \mu\text{m}$) and quartz sand were negative at pH 7 (Table S2). Repulsive electrostatic interaction was thus present between MPs and quartz sand (Fig. S7). Similar as those at pH 5, obvious breakthrough of MPs was observed under all examined solution ionic strength conditions at pH 7. Comparing with the transport of MPs at pH 5 (Fig. 1, left, open symbol), the transport of MPs at pH 7 (Fig. 4, left, open symbol) yet were slightly higher due to the more repulsive interaction between MPs and sand at pH 7 (Fig. S7) relative to pH 5 (Fig. S3). This held true for all three different-sized MPs concerned. Similar as those at pH 5, the MPs transport in porous media slightly decreased with the increase of ionic strength at pH 7, which was agreed with less negative zeta potentials of both MPs and quartz sand (Table S2) and consistent with the DLVO theory (Fig. S7). The decreased MPs transport in porous media with the increase of ionic strength under unfavorable conditions has also been reported previously (Dong et al., 2019; Li et al., 2018).

Similar as those observed at pH 5, MPs BTCs with $n\text{TiO}_2$ (Fig. 4, left, solid symbol) were also lower than without $n\text{TiO}_2$ (Fig. 4, left, open symbol) in all NaCl solutions (0.1, 1 and 10 mM). The decreased transport of MPs with copresence of $n\text{TiO}_2$ was acquired for all three-sized MPs. For instance, ~95% of $1 \mu\text{m}$ MPs in the absence of $n\text{TiO}_2$ passed through the columns in 1 mM NaCl solutions, while percentage decreased to ~60% with $n\text{TiO}_2$ copresent in suspensions at the same ionic strength condition. The observation clearly demonstrated that regardless their negative surface charge at pH 7, the copresence of $n\text{TiO}_2$ also inhibited the transport of all three different-sized MPs in all three NaCl solutions (0.1–10 mM) at pH 7.

Due to the high mobility in 0.1 mM NaCl solutions at pH 7, the amounts of retained MPs for all three different sizes were negligible at this solution condition (Fig. 4, right, open circle). Similar as those at pH 5, the retained concentrations of MPs also increased with increasing ionic strength at pH 7, which was consistent with less surface charge at higher ionic strength and lower pH (Table S2) and thus agreed with DLVO theory (Fig. S7). Moreover, the amounts of MPs with $n\text{TiO}_2$ retained in columns were higher than those without $n\text{TiO}_2$, which held true for all MPs in all examined NaCl solutions (Fig. 4, right, solid symbols vs. open symbols). The results confirmed that $n\text{TiO}_2$ present in suspension also enhanced MPs (all three sizes) deposition in porous media at pH 7. Interestingly, the increased retention of all three different-sized MPs with $n\text{TiO}_2$

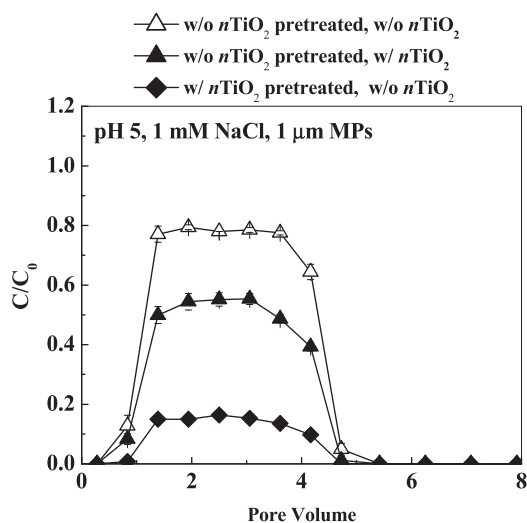


Fig. 3. Breakthrough curves of MPs in 1 mM NaCl solutions at pH 5 only with $n\text{TiO}_2$ present in MPs suspensions (solid triangle) and without $n\text{TiO}_2$ in MPs suspensions while with (solid diamond) and without (open triangle) pre-equilibrating the quartz sand by $n\text{TiO}_2$.

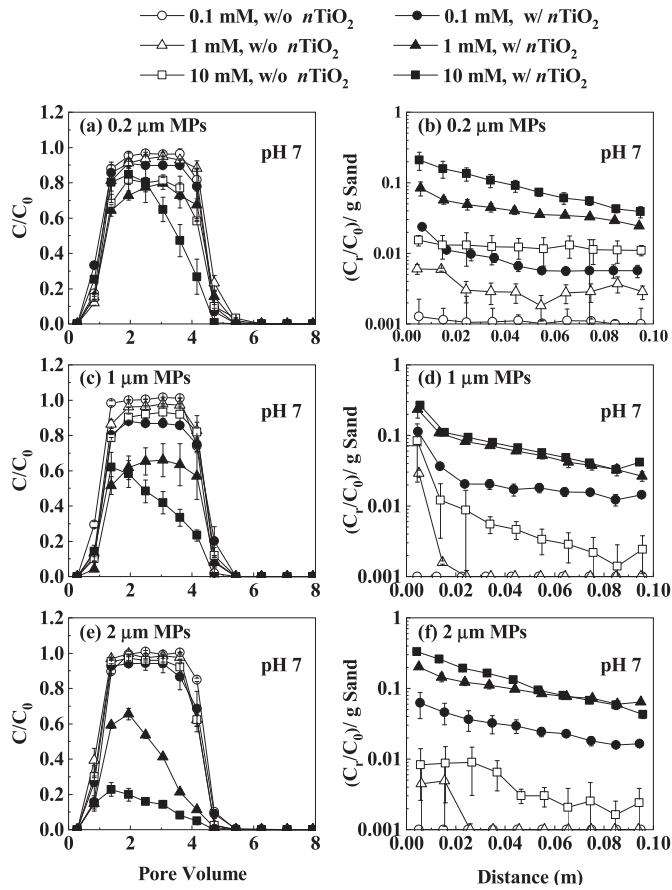


Fig. 4. Breakthrough curves and retained profiles of MPs (0.2, 1 and 2 μm) both with $n\text{TiO}_2$ and without $n\text{TiO}_2$ in suspensions in NaCl solutions (0.1, 1, and 10 mM) at pH 7.

copresent in suspensions also distributed the entire column at pH 7. Unlike those at pH 5, retained profiles of MPs with $n\text{TiO}_2$ at pH 7 yet were mainly in the form of hyper-exponential decrease, which was quite similar as those without $n\text{TiO}_2$. These results suggested that the major mechanisms driving to MPs deposition with $n\text{TiO}_2$ to be similar to those without the $n\text{TiO}_2$ at pH 7.

As stated above, increased colloidal sizes might be one factor driving the increased colloid deposition in porous media (Dong et al., 2018; Legg et al., 2014; Xia et al., 2019). To testify whether the presence of $n\text{TiO}_2$ would also alter the sizes of MPs at pH 7, SEM images (Fig. 5) of MPs with copresence of $n\text{TiO}_2$ in suspensions as well as the number-based size distribution of MPs both with and without $n\text{TiO}_2$ copresent in suspensions (Fig. S8) were acquired. Although $n\text{TiO}_2$ contained negative surface charge, yet adsorption of $n\text{TiO}_2$ onto 1 μm MPs surfaces was also observed in representative solution condition (1 mM) at pH 7 (Fig. 5). Moreover, the size distribution results showed that a slight increase of MPs sizes occurred with the presence of $n\text{TiO}_2$ particles relative to those without $n\text{TiO}_2$ (Fig. S8). Moreover, similar as that observed at pH 5, we also found that the sizes in effluent suspensions of MPs (1 μm) and $n\text{TiO}_2$ mixtures were smaller than that in influent suspensions in 1 mM NaCl solutions at pH 7 (Fig. S6). It is reasonable for us to speculate that the large MPs- $n\text{TiO}_2$ aggregates were easier to be retained in columns, thus the presence of $n\text{TiO}_2$ in suspensions also decreased the transport and increased the deposition of MPs at pH 7. However, comparing with that at pH 5, the change of MPs size with $n\text{TiO}_2$ in suspensions at pH 7 was slight. Thus, it was proposed that the size change was a factor but not the key factor affecting the transport and deposition of MPs with $n\text{TiO}_2$ at pH 7.

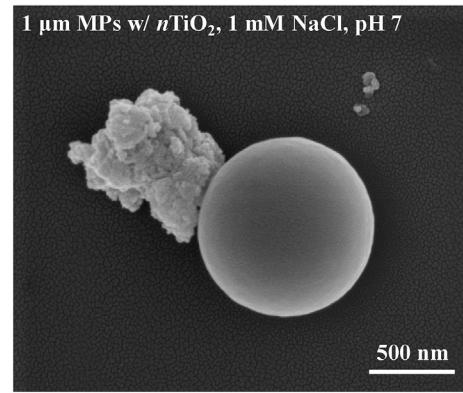


Fig. 5. SEM image of MPs (1 μm) and $n\text{TiO}_2$ mixed suspensions in 1 mM NaCl solutions at pH 7.

It is also reported that the deposition of substances copresent in colloid suspensions onto surfaces of porous media could decrease colloid transport via providing additional sites for colloid deposition even under unfavorable conditions (Chen et al., 2012; Yang et al., 2016). The zeta potentials of $n\text{TiO}_2$ were less negative than quartz sand at pH 7 in present study (Table S2). Electrostatic force between MPs and $n\text{TiO}_2$ thus was less repulsive than that between MPs and quartz sand (Fig. S9 vs. Fig. S7). Comparing with bare quartz sand, MPs might be more likely to deposit on $n\text{TiO}_2$ pre-deposited onto quartz sand surfaces, decreasing MPs transport in quartz sand. To testify, experiments with pre-equilibrating the quartz sand by 3 PVs 50 mg L^{-1} $n\text{TiO}_2$ suspensions before 1 μm MPs transport experiment were conducted at pH 7 in 1 mM NaCl conditions (Fig. 6). MPs BTCs for columns pre-equilibrated by $n\text{TiO}_2$ and followed by individual MPs transport experiment ($\sim 47\%$ breakthrough) (Fig. 6, solid diamond) were lower than that of individual MPs transport experiment without pre-covering sand with $n\text{TiO}_2$ ($\sim 62\%$ breakthrough) (Fig. 6, solid triangle). The results suggested that $n\text{TiO}_2$ pre-deposited onto quartz sand did increase MPs deposition at pH 7. It is expected that the amount of $n\text{TiO}_2$ pre-deposited onto quartz sand surfaces during pre-equilibration process would be greater than that copresent in MPs suspensions. Thereby, MPs BTC for columns only with $n\text{TiO}_2$ pre-covered quartz sand (without $n\text{TiO}_2$ during transport experiment) (Fig. 6, solid

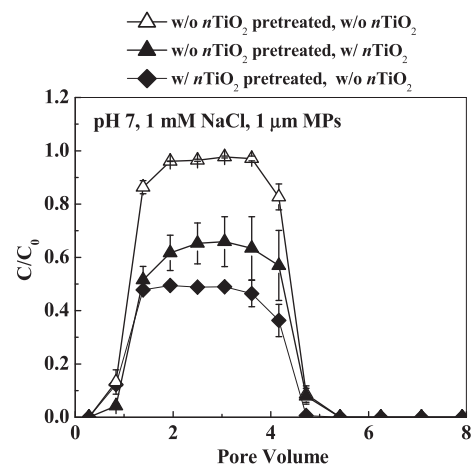


Fig. 6. Breakthrough curves of MPs in 1 mM NaCl solutions at pH 7 only with $n\text{TiO}_2$ copresent in MPs suspensions (solid triangle) and without $n\text{TiO}_2$ in MPs suspensions yet with (solid diamond) and without (open triangle) pre-equilibrating the quartz sand by $n\text{TiO}_2$.

diamond) was lower than that only with $n\text{TiO}_2$ in MPs suspensions (without $n\text{TiO}_2$ pre-covering sand) (Fig. 6, solid triangle). The above results verified that additional sites provided by $n\text{TiO}_2$ deposited onto sand surfaces has contribution to the increase the deposition and decreased transport of MPs with copresence of $n\text{TiO}_2$ at pH 7. In addition, it was recently shown that the presence of nanoscale roughness could largely reduce or sometimes eliminate energy barrier among colloids and porous media (Bradford et al., 2017). Therefore, we proposed that the nanoscale roughness formed by the $n\text{TiO}_2$ deposited on sand surfaces might also contribute to the enhanced deposition of MPs at pH 7 under unfavorable conditions in current study.

4. Conclusion

To figure out the effects of both positive charged and negative charged $n\text{TiO}_2$ nanoparticles on the transport of MPs in porous media, the transport experiments of three different-sized MPs (0.2–2 μm) both with and without the copresence of $n\text{TiO}_2$ nanoparticles were performed under three different ionic strength conditions in NaCl solutions (0.1, 1 and 10 mM) at both pH 5 and 7. Both the BTCs and retained profiles of all different-sized MPs under different solution conditions were acquired. Results showed that for all three different-sized MPs, either positive charged or negative charged $n\text{TiO}_2$ copresent in suspensions could decrease MPs transport and increase their deposition under all examined conditions. The formation of MPs- $n\text{TiO}_2$ clusters and the additional deposition sites via pre-deposited positive charged $n\text{TiO}_2$ onto quartz sand surfaces were responsible for the increased all three different-sized MPs deposition with $n\text{TiO}_2$ copresent in suspensions at pH 5. While the formation of MPs- $n\text{TiO}_2$ aggregates, additional deposition sites and increased surface roughness induced by the pre-deposited $n\text{TiO}_2$ on quartz sand surfaces contributed to the enhanced MPs deposition at pH 7. Although transport experiments were conducted only for spherical polystyrene MPs, the results in present study showed that the copresent $n\text{TiO}_2$ nanomaterial regardless of their surface charge did greatly affect MPs transport in porous media. To fully understand the environmental fate and ecological risks of MPs, the effects of other copresent colloids in natural environment (e.g., engineered nanomaterials) on MPs transport/deposition behaviors should be considered.

Acknowledgment

This work was supported by Beijing Natural Science Foundation under Grant No. JQ18030 and National Natural Science Foundation of China under Grant No.51779001 and 41601518.

Appendix A. Supplementary data

Supplementary data to this article can be found online at <https://doi.org/10.1016/j.envpol.2019.07.006>.

Declaration of interests

The authors declare that they have no known competing financial interests or personal relationships that could have appeared to influence the work reported in this paper.

References

- Alimi, O.S., Farner Budarz, J., Hernandez, L.M., Tufenkji, N., 2018. Microplastics and nanoplastics in aquatic environments: aggregation, deposition, and enhanced contaminant transport. *Environ. Sci. Technol.* 52, 1704–1724.
- Bradford, S.A., Torkzaban, S., Walker, S.L., 2007. Coupling of physical and chemical mechanisms of colloid straining in saturated porous media. *Water Res.* 41, 3012–3024.
- Bradford, S.A., Kim, H., Shen, C., Sasidharan, S., Shang, J., 2017. Contributions of nanoscale roughness to anomalous colloid retention and stability behavior. *Langmuir* 33, 10094–10105.
- Brennecke, D., Duarte, B., Paiva, F., Caçador, I., Canning-Clode, J., 2016. Microplastics as vector for heavy metal contamination from the marine environment. *Estuar. Coast Shelf Sci.* 178, 189–195.
- Browne, M.A., Galloway, T., Thompson, R., 2007. Microplastic—an emerging contaminant of potential concern? *Integr. Environ. Assess. Manag.* 3, 559–561.
- Cai, L., Tong, M., Ma, H., Kim, H., 2013. Cotransport of titanium dioxide and fullerene nanoparticles in saturated porous media. *Environ. Sci. Technol.* 47, 5703–5710.
- Cai, L., Hu, L., Shi, H., Ye, J., Zhang, Y., Kim, H., 2018. Effects of inorganic ions and natural organic matter on the aggregation of nanoplastics. *Chemosphere* 197, 142–151.
- Chen, J.Y., Ko, C.-H., Bhattacharjee, S., Elimelech, M., 2001. Role of spatial distribution of porous medium surface charge heterogeneity in colloid transport. *Colloid. Surf. Physicochem. Eng. Asp.* 191, 3–15.
- Chen, G.X., Liu, X.Y., Su, C.M., 2012. Distinct effects of humic acid on transport and retention of TiO_2 rutile nanoparticles in saturated sand columns. *Environ. Sci. Technol.* 46, 7142–7150.
- Cheung, P.K., Fok, L., 2016. Evidence of microbeads from personal care product contaminating the sea. *Mar. Pollut. Bull.* 109, 582–585.
- de Souza Machado, A.A., Kloas, W., Zarfl, C., Hempel, S., Rillig, M.C., 2018. Microplastics as an emerging threat to terrestrial ecosystems. *Glob. Chang. Biol.* 24, 1405–1416.
- Dong, Z., Qiu, Y., Zhang, W., Yang, Z., Wei, L., 2018. Size-dependent transport and retention of micron-sized plastic spheres in natural sand saturated with seawater. *Water Res.* 143, 518–526.
- Dong, Z., Zhang, W., Qiu, Y., Yang, Z., Wang, J., Zhang, Y., 2019. Cotransport of nanoplastics (NPs) with fullerene (C_{60}) in saturated sand: effect of NPs/ C_{60} ratio and seawater salinity. *Water Res.* 148, 469–478.
- Eerkes-Medrano, D., Thompson, R.C., Aldridge, D.C., 2015. Microplastics in freshwater systems: a review of the emerging threats, identification of knowledge gaps and prioritisation of research needs. *Water Res.* 75, 63–82.
- Elimelech, M., Nagai, M., Ko, C.-H., Ryan, J.N., 2000. Relative insignificance of mineral grain zeta potential to colloid transport in geochemically heterogeneous porous media. *Environ. Sci. Technol.* 34, 2143–2148.
- Erickson, B., 2012. Nanomaterials in food, cosmetics. *Chem. Eng. News* 90, 8.
- Gottschalk, F., Sun, T., Nowack, B., 2013. Environmental concentrations of engineered nanomaterials: review of modeling and analytical studies. *Environ. Pollut.* 181, 287–300.
- Hernandez, L.M., Yousefi, N., Tufenkji, N., 2017. Are there nanoplastics in your personal care products? *Environ. Sci. Technol. Lett.* 4, 280–285.
- Ivleva, N.P., Wiesheu, A.C., Niessner, R., 2017. Microplastic in aquatic ecosystems. *Angew. Chem. Int. Ed.* 56, 1720–1739.
- Keller, A.A., Lazareva, A., 2013. Predicted releases of engineered nanomaterials: from global to regional to local. *Environ. Sci. Technol. Lett.* 1, 65–70.
- Kim, S.-B., Park, S.-J., Lee, C.-G., Choi, N.-C., Kim, D.-J., 2008. Bacteria transport through goethite-coated sand: effects of solution pH and coated sand content. *Colloids Surfaces B Biointerfaces* 63, 236–242.
- Legg, B.A., Zhu, M.Q., Comolli, L.R., Gilbert, B., Banfield, J.F., 2014. Impacts of ionic strength on three-dimensional nanoparticle aggregate structure and consequences for environmental transport and deposition. *Environ. Sci. Technol.* 48, 13703–13710.
- Li, M., He, L., Zhang, M.Y., Liu, X.W., Tong, M.P., Kim, H., 2019. Cotransport and deposition of iron oxides with different-sized plastic particles in saturated quartz sand. *Environ. Sci. Technol.* 53, 3547–3557.
- Li, S., Liu, H., Gao, R., Abdurahman, A., Dai, J., Zeng, F., 2018. Aggregation kinetics of microplastics in aquatic environment: complex roles of electrolytes, pH, and natural organic matter. *Environ. Pollut.* 237, 126–132.
- Li, W.C., Tse, H.F., Fok, L., 2016. Plastic waste in the marine environment: a review of sources, occurrence and effects. *Sci. Total Environ.* 566–567, 333–349.
- Lin, D., Tian, X., Wu, F., Xing, B., 2010. Fate and transport of engineered nanomaterials in the environment. *J. Environ. Qual.* 39, 1896–1908.
- Mueller, N.C., Nowack, B., 2008. Exposure modeling of engineered nanoparticles in the environment. *Environ. Sci. Technol.* 42, 4447–4453.
- Mueller, N.C., Nowack, B., 2010. Nanoparticles for remediation: solving big problems with little particles. *Elements* 6, 395–400.
- Napper, I.E., Thompson, R.C., 2016. Release of synthetic microplastic plastic fibres from domestic washing machines: effects of fabric type and washing conditions. *Mar. Pollut. Bull.* 112, 39–45.
- Pitt, J.A., Kozal, J.S., Jayasundara, N., Massarsky, A., Trevisan, R., Geitner, N., Wiesner, M., Levin, E.D., Di Giulio, R.T., 2018. Uptake, tissue distribution, and toxicity of polystyrene nanoparticles in developing zebrafish (*Danio rerio*). *Aquat. Toxicol.* 194, 185–194.
- Rochman, C.M., Kurobe, T., Flores, I., Teh, S.J., 2014. Early warning signs of endocrine disruption in adult fish from the ingestion of polyethylene with and without sorbed chemical pollutants from the marine environment. *Sci. Total Environ.* 493, 656–661.
- Ter, H.A., Ladirat, L., Gendre, X., Goudounèche, D., Pusineri, C., Routaboul, C., Tenailleau, C., Duployer, B., Perez, E., 2016. Understanding the fragmentation pattern of marine plastic debris. *Environ. Sci. Technol.* 50, 5668.
- Tong, M., Johnson, W.P., 2007. Colloid population heterogeneity drives hyper-exponential deviation from classic filtration theory. *Environ. Sci. Technol.* 41, 493–499.

- Turner, A., 2016. Heavy metals, metalloids and other hazardous elements in marine plastic litter. *Mar. Pollut. Bull.* 111, 136–142.
- Wang, X., Cai, L., Han, P., Lin, D., Kim, H., Tong, M., 2014. Cotransport of multi-walled carbon nanotubes and titanium dioxide nanoparticles in saturated porous media. *Environ. Pollut.* 195, 31–38.
- Wang, Z., Chen, M., Zhang, L., Wang, K., Yu, X., Zheng, Z., Zheng, R., 2018. Sorption behaviors of phenanthrene on the microplastics identified in a mariculture farm in Xiangshan Bay, southeastern China. *Sci. Total Environ.* 628–629, 1617–1626.
- Wardrop, P., Shimeta, J., Nugegoda, D., Morrison, P.D., Miranda, A., Tang, M., Clarke, B.O., 2016. Chemical pollutants sorbed to ingested microbeads from personal care products accumulate in fish. *Environ. Sci. Technol.* 50, 4037–4044.
- Xia, T.J., Ma, P.K., Qi, Y., Zhu, L.Y., Qi, Z.C., Chen, W., 2019. Transport and retention of reduced graphene oxide materials in saturated porous media: synergistic effects of enhanced attachment and particle aggregation. *Environ. Pollut.* 247, 383–391.
- Yang, H., Ge, Z., Wu, D., Tong, M., Ni, J., 2016. Cotransport of bacteria with hematite in porous media: effects of ion valence and humic acid. *Water Res.* 88, 586–594.
- Yao, K.M., Habibian, M.M., Omelia, C.R., 1971. Water and waste water filtration - concepts and applications. *Environ. Sci. Technol.* 5, 1105.
- Zhang, K., Xiong, X., Hu, H., Wu, C., Bi, Y., Wu, Y., Zhou, B., Lam, P.K.S., Liu, J., 2017. Occurrence and characteristics of microplastic pollution in xiangxi bay of three gorges reservoir, China. *Environ. Sci. Technol.* 51, 3794–3801.